



Fast heterogeneous N_2O_5 uptake and ClNO_2 production in power plant plumes observed in the nocturnal residual layer over the North China Plain

Zhe Wang¹, Weihao Wang¹, Yee Jun Tham^{1, a}, Qinyi Li¹, Hao Wang², Liang Wen², Xinfeng Wang²,
5 Tao Wang¹

¹Department of Civil and Environmental Engineering, The Hong Kong Polytechnic University, Hong Kong, China

²Environment Research Institute, Shandong University, Jinan, China

^aNow at: Department of Physics, University of Helsinki, Finland

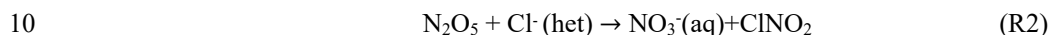
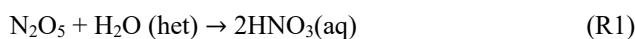
10 *Correspondence to:* Zhe Wang (z.wang@polyu.edu.hk), Tao Wang (cetwang@polyu.edu.hk)

Abstract. Dinitrogen pentoxide (N_2O_5) and nitryl chloride (ClNO_2) are key species in nocturnal tropospheric chemistry, and have significant effects on particulate nitrate formation and the following day's photochemistry. To better understand the roles of N_2O_5 and ClNO_2 in the high aerosol loading environment of northern China, an intensive field study was carried out at a high-altitude site (Mt. Tai, 1465 m a.s.l) in the North China Plain (NCP) during the summer of 2014. Elevated ClNO_2 plumes
15 were frequently observed in the nocturnal residual layer with a maximum mixing ratio of 2.1 ppbv (1-min), whilst N_2O_5 was typically present at very low levels (<30 pptv), indicating fast heterogeneous N_2O_5 hydrolysis. Combined analyses of chemical characteristics and backward trajectories indicated that the ClNO_2 -laden air was caused by the transport of NO_x -rich plumes from the coal-fired power plants in the NCP. The heterogeneous N_2O_5 uptake coefficient (γ) and ClNO_2 yield (ϕ) during the campaign exhibited high variability, with means of 0.061 ± 0.025 and 0.27 ± 0.24 , respectively. These derived values are
20 higher than those derived from previous laboratory and field studies in other regions, and cannot be well characterized by model parameterizations. Fast heterogeneous N_2O_5 reactions dominated the nocturnal NO_x loss in the residual layer over this region, and contributed to substantial nitrate formation of up to $17 \mu\text{g m}^{-3}$. The determined nocturnal nitrate formation rates ranged from 0.2 to $4.8 \mu\text{g m}^{-3} \text{ hr}^{-1}$ in various plumes, with a mean of $2.2 \pm 1.4 \mu\text{g m}^{-3} \text{ h}^{-1}$. The results demonstrate the significance of heterogeneous N_2O_5 reactivity and chlorine activation in the NCP, and their unique and universal roles in fine
25 aerosol formation and NO_x transformation, and thus potential impacts on regional haze pollution in northern China.



1 Introduction

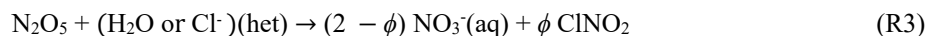
Nitrogen oxides ($\text{NO}_x = \text{NO} + \text{NO}_2$) plays central roles in the oxidative capacity of the atmosphere and photochemical air pollution. Dinitrogen pentoxide (N_2O_5) is an important reactive intermediate in the oxidation of NO_x , and exists in rapid thermal equilibrium with nitrate radical (NO_3) formed via the reaction between NO_2 and O_3 . The heterogeneous hydrolysis of N_2O_5 has been recognized as a key step in nocturnal NO_x removal, and can affect regional air quality by regulating the reactive nitrogen budget and nitrate aerosol formation (e.g., Brown et al., 2006; Abbatt et al., 2012). The heterogeneous reaction of N_2O_5 on and within atmospheric aerosols, fog or cloud droplets, produces soluble nitrate (HNO_3 or NO_3^-) and nitryl chloride (ClNO_2) when chloride is available in the aerosols (Finlayson-Pitts et al., 1989).



The rate coefficient of the heterogeneous N_2O_5 reactions is governed by the available reaction surface and N_2O_5 reaction probability (also known as the uptake coefficient $\gamma_{\text{N}_2\text{O}_5}$), and can be described by the following expression when the gas-phase diffusive effect is negligible.

$$k(\text{N}_2\text{O}_5)_{\text{het}} = \frac{1}{4} c_{\text{N}_2\text{O}_5} \gamma_{\text{N}_2\text{O}_5} S_a \quad (1)$$

Here, $c_{\text{N}_2\text{O}_5}$ is the mean molecular speed of N_2O_5 , and S_a is the aerosol (or cloud) surface area density. The yield of ClNO_2 (ϕ) is defined as the amount of ClNO_2 formed per loss of N_2O_5 , representing the fraction to ClNO_2 formation. Hence, the net reaction of R1 and R2 can be written as follows:



The $\gamma_{\text{N}_2\text{O}_5}$ has been experimentally measured on various types of aerosols surfaces (including sulfate, nitrate, black carbon, organic carbon, organic coating sulfate, sea salts, and dust, etc.) in the laboratory, and different parameterizations based on aerosol composition have been proposed in varying degree of complexity (e.g., Evans and Jacob, 2005; Anttila et al., 2006; Davis et al., 2008; Bertram and Thornton, 2009; Griffiths et al., 2009; Riemer et al., 2009; Roberts et al., 2009; Simon et al., 2009; Foley et al., 2010; Chang et al., 2011; Ammann et al., 2013; Tang et al., 2014). Recently, field studies have been carried out to measure ambient N_2O_5 and to derive the $\gamma_{\text{N}_2\text{O}_5}$ from atmospheric observations (e.g., Bertram et al., 2009b; Brown et al., 2009; Morgan et al., 2015; Brown et al., 2016; Chang et al., 2016; Phillips et al., 2016). These field-derived/measured $\gamma_{\text{N}_2\text{O}_5}$ values were found to vary considerably, and the observed range to be significantly larger than that from laboratory studies using synthetic aerosols (Chang et al., 2011; Phillips et al., 2016). Furthermore, inconsistencies between $\gamma_{\text{N}_2\text{O}_5}$ values derived from field measurements and parameterizations were observed in some locations, which implies that $\gamma_{\text{N}_2\text{O}_5}$ has a complex dependence on the aerosol composition, physico-chemical characteristics, and environmental parameters (Chang et al., 2011 and references therein). Similarly, for the ClNO_2 yield, the field-determined values exhibited significant variability, ranging from 0.01 to close to unity (Thornton et al., 2010; Riedel et al., 2013; Wagner et al., 2013; Phillips et al., 2016), which could



not be well reproduced (exhibiting a tenfold difference in some cases) by parameterization based on only aerosol chloride and water content (Wagner et al., 2013; Wang et al., 2017b). The field determination of ϕ is still limited, and the possible effects of real atmospheric aerosols (including organic composition, mixing state, and chloride partitioning between particle sizes, etc.) have not been well characterized (Mielke et al., 2013; Phillips et al., 2016). This incomplete understanding suggests the
5 necessity of more field measurements of γ and ϕ in various environments, to facilitate the validation and construction of parameterizations suitable for use in air quality models.

CINO₂ formed from nocturnal heterogeneous N₂O₅ uptake can potentially affect the atmospheric oxidative capacity via the production of highly reactive chlorine radicals (Cl) and the recycling of NO_x after photolysis (Simpson et al., 2015). Elevated CINO₂ mixing ratios were firstly observed in several polluted coast regions (for instance, the coasts of Texas and California,
10 and the Los Angeles Basin), resulting from the strong emission of NO_x and abundant chloride from sea salt aerosols (Osthoff et al., 2008; Riedel et al., 2012; Mielke et al., 2013). Recently, significant CINO₂ production was also observed in some inland areas (such as Colorado, Hessen, and Canada), with mixing ratio up to several hundreds of pptv or even exceeding 1.0 ppbv (e.g., Mielke et al., 2011; Phillips et al., 2012; Riedel et al., 2013; Faxon et al., 2015). Anthropogenic sources of chlorine including coal combustion in power plants, industries, and biomass burning may potentially facilitate CINO₂ production. The
15 highest CINO₂ mixing ratio yet reported (4.7 ppbv) was recently observed in the regional plumes at a mountaintop site in southern China, indicating the importance of N₂O₅/CINO₂ chemistry in polluted environments (Wang et al., 2016).

Large anthropogenic emissions of NO_x and increasing O₃ concentrations have been reported in many urban cluster regions in China (Wang et al., 2006; Wang et al., 2017a). Hence, in these regions, nocturnal nitrogen chemistry may be particularly important in the transformation of NO_x and the subsequent effects on daytime photochemistry and secondary aerosol formation.
20 In the areas downwind of Beijing and Shanghai, high concentrations of particulate nitrate (up to 40 $\mu\text{g m}^{-3}$) have been observed and attributed to heterogeneous N₂O₅ uptake on acidic aerosols (Pathak et al., 2009; Pathak et al., 2011). During a more recent field study in a rural site in the North China Plain (NCP), elevated fine nitrate concentrations were observed at night and in the early morning, with hourly maxima of up to 87.2 $\mu\text{g m}^{-3}$ and a 30% contribution to PM_{2.5}, which was mainly attributed to the heterogeneous hydrolysis of N₂O₅ (Wen et al., 2015). Active heterogeneous N₂O₅ chemistry has been recently characterized
25 in both rural and urban areas of the NCP via direct measurements of N₂O₅ and CINO₂. Rapid heterogeneous N₂O₅ loss and efficient CINO₂ production were observed, with a maximum CINO₂ mixing ratio of 2.07 ppbv at Wangdu and 0.77 ppbv at Jinan (Tham et al., 2016; Wang et al., 2017b). Moreover, sustained CINO₂ peaks were observed after sunrise in the region, and the downward mixing of CINO₂-rich air in the residual layer was proposed to be the cause of morning peaks (Tham et al., 2016). To confirm these findings and better characterize the chemistry of N₂O₅/CINO₂ and their impacts on regional air quality,
30 it is of great interest to conduct direct field measurements of N₂O₅/CINO₂ in the polluted residual layer.

In the present study, we measured the concentrations of N₂O₅, CINO₂, and related species at a mountaintop site in the NCP and characterized the nighttime nitrogen chemistry within the residual layer over a polluted region of northern China. We examined the frequently intercepted CINO₂-rich plumes at this high elevation site, and investigated nocturnal N₂O₅ reactivity



to determine the heterogeneous N_2O_5 uptake coefficients and ClNO_2 yields in a variety of air masses, which were also compared to parameterizations utilized in existing models. The effects of heterogeneous N_2O_5 chemistry on particulate nitrate formation and nocturnal NO_x loss were then evaluated based on the observation data.

2. Methodology

5 2.1 Field Study Site

The measurement site was located on Mount Tai (36.25°N, 117.10°E, 1465 m above sea level) in Shandong Province, China. Mt. Tai is located between the two most developed regions in China (Jing-Jin-Ji and the Yangtze River Delta), and its peak (1545 m a.s.l.) is the highest point within the NCP. Figure 1 shows the location of the measurement site in relation to the surrounding topography. The cities of Tai'an and Jinan (the capital of Shandong Province) are located 15 km south and 60 km
10 north of the measurement site, respectively. The altitude of the measurement site is near the top of the boundary layer in the daytime during the summer, and is typically in the residual layer or, occasionally, in the free troposphere at night. This mountaintop site has been previously used in many atmospheric chemistry field studies (e.g., Gao et al., 2005; Wang et al., 2011; Guo et al., 2012; Sun et al., 2016). Although Mt. Tai is a popular location for tourists, the measurement site is located in an area that is not frequently visited and therefore, should not be significantly affected by local anthropogenic emissions.
15 Intensive measurements were performed from July 24 to August 27, 2014. During this period, the prevailing winds originated from the northeast and northwest. Shandong province is the largest producer of thermal power in China, therefore, dozens of coal-fired power plants are situated within a radius of 200 km from the mountain site.

2.2 Instrumentation

N_2O_5 and ClNO_2 were measured concurrently using iodide quadrupole chemical ionization mass spectrometry (CIMS) (THS
20 Instruments Inc., USA). The principle and calibration of this CIMS system have been described previously by Wang et al. (2016) and Tham et al. (2016). The same configuration was used in the present study. Briefly, N_2O_5 and ClNO_2 were detected as $\text{I}(\text{N}_2\text{O}_5)^-$ and $\text{I}(\text{ClNO}_2)^-$ clusters via reaction with iodide ions (I^-), which were generated from a mixture of CH_3I (0.3% v/v) and N_2 using an alpha radioactive source, ^{210}Po (NRD, P-2031-2000). The inlet was installed ~ 1.5 m above the roof of a single-story building, and the sampling line was a 5.5 m PFA-Teflon tubing (1/4 in. o.d.) which was replaced daily and washed
25 in the ultrasonic bath to minimize wall loss caused by deposited particles (Wang et al., 2016). A small proportion (1.7 SLPM) of total sampling flow (~ 11 SLPM) was diverted to the CIMS system, to reduce the residence time of the air samples in the sampling line. Manual calibrations of N_2O_5 and ClNO_2 were conducted daily to monitor the instrument sensitivity and background. The N_2O_5 standard was synthesized on-line from the reaction between NO_2 and O_3 , and the ClNO_2 was produced by passing a known concentration of N_2O_5 through a NaCl slurry. The field background was determined by passing the ambient
30 sample through a filter packed with activated carbon. The detection limit was 4 pptv for both N_2O_5 and ClNO_2 (2σ , 1 min-averaged data).



The related trace gases and aerosol compositions were also measured concurrently during the campaign. All of the instruments were used in our previous field studies, and the setup, precision, and accuracies of these instruments were described previously (Wen et al., 2015; Tham et al., 2016; Wang et al., 2016; Wang et al., 2017b). Briefly, NO and NO₂ were measured using a chemiluminescence analyzer equipped with a blue-light converter (TEI, Model 42I-TL). Total gaseous reactive nitrogen (NO_y) was determined using a chemiluminescence analyzer with an external molybdenum oxide (MoO) catalytic converter (TEI, Model 42CY) with an inlet filter. The NO_y described here is different from that in previous reports (Tham et al., 2016; Wang et al., 2016), because that the particulate nitrate was not included but removed by the filter in the present study. O₃, SO₂, and CO were measured using the ultraviolet photometry, pulsed-UV fluorescence, and IR photometry techniques (TEI, Model 49I, 43C and 48C), respectively. Zero and span calibrations for trace gases were performed weekly during the campaign. Water-soluble ionic compositions of PM_{2.5} (including NH₄⁺, Na⁺, Ca²⁺, Mg²⁺, Cl⁻, SO₄²⁻, and NO₃⁻) were measured hourly by a Monitor for Aerosols and Gases (MARGA ADI 2080, Applikon-ECN) using on-line ion chromatography.

The particle number and size distribution (5 nm to 10 μm) were measured using a Wide-Range Particle Spectrometer (WPS, Model 1000XP, MSP Corporation, USA). The particle diameters were corrected for particle hygroscopicity to determine the actual ambient aerosol surface density, and the wet diameters were calculated using growth factors from a size-resolved kappa-Köhler function obtained in a rural site in the NCP (Ma et al., 2016; Tham et al., 2016). Meteorological data, including temperature, relative humidity (RH), wind vectors and photolysis frequency of NO₂ (J_{NO_2}) were measured by an automated meteorological station (JZYG, PC-4) and a filter radiometer (Metcon, Germany). In addition, a Lagrangian particle dispersion model, Hybrid Single-Particle Lagrangian Integrated Trajectory (HYSPLIT) model (Draxler and Hess, 1998; Wang et al., 2016), driven by high spatial and temporal meteorological fields from the WRF model, was used to investigate potential source regions of the air masses intercepted at the measurement site. The HYSPLIT model was run 12-h backward with 2500 particles released at the measurement site. Detailed parameterization and setup of the HYSPLIT and WRF models were previously described by Wang et al. (2016) and Tham et al. (2016).

3. Results and Discussion

3.1 Overview of N₂O₅ and ClNO₂ measurement

The temporal variations of ClNO₂, N₂O₅, related trace gases, and selected meteorological parameters during the field study at Mt. Tai are depicted in Figure 2. Overall, the observed mixing ratios of ClNO₂ were higher than those of N₂O₅, and exhibited significant variations. The average mixing ratios of N₂O₅ and ClNO₂ were 6.8 ± 7.7 pptv and 54 ± 106 pptv, respectively. The maximum mixing ratio of N₂O₅ (167 pptv) was observed at 21:00 on August 26, 2014, and most of the other nights during the observation period exhibited peak N₂O₅ mixing ratios below 30 pptv. The average nighttime mixing ratios of O₃ and NO₂ were 77 and 3.0 ppbv, respectively, with an average nitrate radical production rate $p(\text{NO}_3)$ of 0.45 ± 0.40 ppb h⁻¹, which is indicative of potentially active NO₃ and N₂O₅ chemistry during the study period. However, the low N₂O₅ mixing ratios observed during



most of the nights suggest rapid loss of N_2O_5 , via either heterogeneous uptake or via NO_3 loss. The higher RH during nighttime and the frequent occurrence of clouds at the mountaintop site could also account for low N_2O_5 concentrations, because of its rapid heterogeneous loss on cloud droplets.

The highest ClNO_2 mixing ratio of 2065 pptv was observed on August 8, 2014, and on 8 of the 35 nights the peak ClNO_2 mixing ratios were higher than 500 pptv. The simultaneous increases of SO_2 and CO with these ClNO_2 peaks suggest these air masses originated from coal combustion sources, such as power plants, which will be further discussed in the next section. The elevated ClNO_2 levels observed at Mt. Tai are similar to recent measurements at a surface rural site (Wangdu) in northern China (Tham et al., 2016) and a mountain site (Tai Mo Shan) in southern China (Wang et al., 2016), but are slightly higher than previous measurements conducted in coastal (e.g., Osthoff et al., 2008; Riedel et al., 2012; Mielke et al., 2013) and inland sites (e.g., Thornton et al., 2010; Phillips et al., 2012; Riedel et al., 2013) in other regions of the world.

The mean diurnal variations of N_2O_5 , ClNO_2 , and other relevant chemical species during the study period are shown in Figure 3. Ozone exhibited a typical diurnal pattern for a polluted mountaintop site (Sun et al., 2016), and it began to increase in the late morning and reached an afternoon peak of 88.6 ppbv with a daily average rise of 24.4 ppbv. The average O_3 kept at elevated levels after sunset and did not begin to decrease until 22:00, and NO_x exhibited a diel maximum of 6.1 ppbv before sunset, resulting in a peak in $p(\text{NO}_3)$ just before sunset and relatively high levels in the early night. Gaseous NO_y reached a maximum of 16.4 ppbv in the morning, and remained stable at a high level during the daytime; the air masses were more aged during the daytime, as indicated by the persistent low NO_x/NO_y ratios (0.2-0.25). Small N_2O_5 peaks were observed immediately after sunset, resulting from the abundant O_3 and NO_2 , and was present at low levels near to the detection limit of the CIMS throughout the rest of the night. ClNO_2 exhibited clear nighttime elevations resulting from the heterogeneous production after sunset, and reached a diel maximum around midnight. The low N_2O_5 and high ClNO_2 concentrations observed at Mt. Tai are similar to the measurement at a rural surface site within the NCP (Tham et al., 2016), suggesting rapid heterogeneous loss of N_2O_5 and production of ClNO_2 in this region.

3.2 High ClNO_2 plumes from power plants

As described above, several plumes with elevated ClNO_2 concentrations (> 500 pptv) were observed during the measurement period. Figure 4a illustrates the high ClNO_2 case observed during the night of July 30-31, 2014. The ClNO_2 concentration peaked sharply at 1265 pptv, which was accompanied by a steep rise in the concentrations of SO_2 , CO and NO_x , indicating the combustion origin of this plume from power plants. The 12-h backward particle dispersion trajectories calculated from the HYSPLIT model revealed that the air masses mostly moved slowly from the west, and passed over two large power plants before arriving at the measurement site. Figure 5a shows the highest ClNO_2 case (2065 ppbv) observed on the night of August 8, 2014. The simultaneous increases in SO_2 , CO, and NO_x concentrations, together with the derived backward particle dispersion trajectories, again indicate that the air masses originated from the power plants to the west of Mt. Tai. Table 1 summarizes the chemical characteristics of the eight cases of high- ClNO_2 power plant plumes during the study period. In these



cases, the average SO₂ mixing ratios ranged from 2.3 to 18.7 ppbv, and the maximum ClNO₂ and N₂O₅ mixing ratios ranged from 534 to 2065 ppbv and 7.3 to 40.1 ppbv, respectively, with corresponding ClNO₂/N₂O₅ ratios of 25 to 118. The mixing ratios for O₃ and NO₂ ranged from 60 to 106 ppbv and 2.8 to 11.8 ppbv, respectively, resulting in high $p(\text{NO}_3)$ values of 0.60 to 1.59 ppbv h⁻¹.

5 NO_x emissions from the combustion sources such as power plants contain abundant NO, which is oxidized rapidly to NO₂ by ambient O₃. Thus, the anti-correlation between O₃ and NO₂ within the observed plumes (cf. Figure 4b and 5b) can be another indicator of the large combustion sources (such as coal-fired power plant). Furthermore, the slope of a plot of O₃ vs. NO₂ for nighttime plumes can be considered as an approximate measure of the plume age, with the assumption of pseudo-first-order kinetics and when the input of NO_x is small comparing to the excess O₃ (Brown et al., 2006). The estimated plume age can be
10 determined as follows:

$$t_{plumes} \approx \ln(1 - S(m + 1)) / (Sk\bar{O}_3) \quad (2)$$

where m is the derived slope, k is the rate coefficient for the reaction of NO₂ with O₃, \bar{O}_3 is the average O₃ concentration in the plume, and S is a stoichiometric factor that varies between 1 for dominant NO₃ loss and 2 for dominant N₂O₅ loss (Brown et al., 2006). In the present study, heterogeneous N₂O₅ uptake dominated the reactive nitrogen loss, therefore $S = 2$ was used in
15 the calculation. The plume ages for the July 30-31 and August 8 cases were calculated to be 3.2 and 2.1 h, respectively, which are consistent with the moderate NO_x/NO_y ratios of 0.4-0.5, and comparable to those observed in nocturnal power plant plumes in the eastern coast of the USA (Brown et al., 2006; Brown et al., 2007). The slopes of O₃ vs. NO₂ in Figure 4b and 5b steeper than 1.0 also indicate the further reactions of NO₂ with O₃, which favor the formation of NO₃ and N₂O₅. However, the N₂O₅ concentrations only showed a slight increase (Figure 4 case) or no apparent change (Figure 5 case), in contrast to the significant
20 increases in ClNO₂ and high $p(\text{NO}_3)$ values, which suggests rapid heterogeneous loss of N₂O₅ and significant ClNO₂ production during transport of these plumes from their sources.

The elevated ClNO₂ concentrations in power plant plumes here are comparable to previous observation of power plant plumes via tower measurements in Colorado (Riedel et al., 2013) and at a mountain site in southern China (Wang et al., 2016), but the observed N₂O₅ within the plumes are significantly lower than those in other power plant plumes observed via aircraft, tower,
25 and at mountain sites (Brown et al., 2007; Riedel et al., 2013; Brown et al., 2016). The previous measurement at a surface site in the NCP has observed sustained ClNO₂ peaks after sunrise, which was proposed to be the cause of the downward mixing of ClNO₂-rich air (estimated values of 1.7-4.0 ppbv) in the residual layer (Tham et al., 2016). In the present study, the frequent intercepts of power plant plumes with elevated ClNO₂ concentrations at Mt. Tai, which were typically above the nocturnal boundary layer, affirm this hypothesis and provide direct evidence that significant ClNO₂ production occurred in the residual
30 layer from the abundant nocturnal NO_x, chloride and background O₃ over the NCP. The similar ClNO₂-laden air frequently observed at high-elevation sites in northern and southern China suggest ubiquitous ClNO₂ in the polluted residual layer and its importance in the daytime production of ozone in China (Tham et al., 2016; Wang et al., 2016). Moreover, the concurrent



nitrate production from heterogeneous N_2O_5 reactions (cf. R3) may also contribute to the formation of haze pollution in these regions.

3.3 N_2O_5 reactivity and heterogeneous uptake coefficient

3.3.1 Reactivity of N_2O_5 and NO_3

- 5 The mixing ratios of N_2O_5 depend on the nitrate radical production rate and the reactivity of N_2O_5 and NO_3 , including the individual loss rates for N_2O_5 or NO_3 that contribute to the removal of the pair. N_2O_5 reactivity can be assessed using the inverse N_2O_5 steady state lifetime, which is the ratio of $p(\text{NO}_3)$ to the observed N_2O_5 mixing ratios (e.g., Brown et al., 2006; Brown et al., 2009; Brown et al., 2016):

$$\tau(\text{N}_2\text{O}_5)^{-1} = \frac{p(\text{NO}_3)}{[\text{N}_2\text{O}_5]} \approx \frac{k(\text{NO}_3)}{K_{eq}[\text{NO}_2]} + k(\text{N}_2\text{O}_5)_{\text{het}} \quad (3)$$

- 10 The steady state inverse lifetime of N_2O_5 , $\tau(\text{N}_2\text{O}_5)^{-1}$, is the sum of the N_2O_5 loss rate via heterogeneous loss ($k(\text{N}_2\text{O}_5)_{\text{het}}$) and NO_3 reactions with VOCs ($k(\text{NO}_3)$) with a ratio of $K_{eq}[\text{NO}_2]$. K_{eq} is the temperature-dependent N_2O_5 - NO_3 equilibrium coefficient. High N_2O_5 reactivity was observed in the present study, with average nighttime $\tau(\text{N}_2\text{O}_5)^{-1}$ of $1.41 \times 10^{-2} \text{ s}^{-1}$ before
15 midnight and $1.30 \times 10^{-2} \text{ s}^{-1}$ after midnight, corresponding to a nighttime N_2O_5 lifetime of 1.2-1.3 min. This rapid N_2O_5 loss rate is comparable to the results from surface measurements in both urban and rural sites in the NCP (Tham et al., 2016; Wang et al., 2017b). However, this loss rate is significantly higher than those determined from a mountain site in southern China (Brown et al., 2016) and tower and aircraft measurements in the USA (e.g., Brown et al., 2009; Wagner et al., 2013).

The NO_3 reactivity, or loss rate coefficient $k(\text{NO}_3)$, can be estimated from the sum of the products of measured VOC concentrations and the bimolecular rate coefficients for the corresponding NO_3 -VOC reactions (Atkinson and Arey, 2003):

$$k(\text{NO}_3) = k_{\text{NO}+\text{NO}_3}[\text{NO}] + \sum_i k_i [\text{VOC}_i] \quad (4)$$

- 20 Because of the lack of concurrent VOCs measurements in the present study, we used the average VOC speciations measured before sunrise and in the evening at Mt. Tai during our previous study in 2007 (c.f. Table S1) to estimate $k(\text{NO}_3)$. The determined nighttime $k(\text{NO}_3)$ was $1.33 \times 10^{-2} \text{ s}^{-1}$ for the first half of the night and $1.07 \times 10^{-2} \text{ s}^{-1}$ for the period after midnight, which is equivalent to an NO_3 lifetime of approximately 1.5 min.

- Figure 6a shows the averaged total N_2O_5 reactivity and fractions of N_2O_5 loss via NO_3 and heterogeneous N_2O_5 loss during the
25 study period. As shown, the heterogeneous loss was dominant, accounting for 80% and 71% of total N_2O_5 reactivity before and after midnight, respectively. Figure 6b shows the contribution of different VOC categories to the average first-order NO_3 loss rate coefficients, $k(\text{NO}_3)$. Biogenic monoterpenes accounted for more than half of the NO_3 reactivity, followed by anthropogenic alkenes (such as butene), isoprene and dimethyl sulfide (DMS). Aromatics and alkanes made small contributions (<1%) to the total NO_3 reactivity. The dominant contribution to NO_3 reactivity from biogenic VOCs is similar
30 to that observed from a mountain site in southern China (Brown et al., 2016), but the absolute value of NO_3 reactivity and the



anthropogenic contribution are much higher in the present study. The estimated NO_3 activity is slightly lower than that obtained from surface site measurements in the NCP (Tham et al., 2016; Wang et al., 2017b), which is in line with the higher abundances of VOCs in the polluted boundary layer.

3.3.2 N_2O_5 uptake coefficient

5 Because the N_2O_5 uptake coefficient γ is related to the first-order loss rate coefficient of N_2O_5 , $k(\text{N}_2\text{O}_5)_{\text{het}}$ (Eq. (1)), then the Eq. (3) can be expressed as follows:

$$\tau(\text{N}_2\text{O}_5)^{-1} K_{\text{eq}}[\text{NO}_2] \approx k(\text{NO}_3) + \frac{1}{4} c_{\text{N}_2\text{O}_5} S_a K_{\text{eq}}[\text{NO}_2] \gamma(\text{N}_2\text{O}_5) \quad (5)$$

The linear relationship between the left-hand side of Eq. (5) and $1/4 c_{\text{N}_2\text{O}_5} S_a K_{\text{eq}}[\text{NO}_2]$ will give the N_2O_5 uptake coefficient γ as the slope, and the NO_3 loss rate coefficient $k(\text{NO}_3)$ as the intercept (Brown et al., 2009). We selected data for periods in which $d[\text{N}_2\text{O}_5]/dt$ is close to zero and the lifetime is relatively stable, which best correspond to steady-state conditions. Figure 7 shows two examples of $\tau(\text{N}_2\text{O}_5)^{-1} K_{\text{eq}}[\text{NO}_2]$ versus $1/4 c_{\text{N}_2\text{O}_5} S_a K_{\text{eq}}[\text{NO}_2]$ for cases observed on the nights of August 2 and 21, 2014. The γ and $k(\text{NO}_3)$ values derived from the linear fits are $\gamma = 0.040$ and $k(\text{NO}_3) = 0.025 \text{ s}^{-1}$ for August 2 case and $\gamma = 0.078$ and $k(\text{NO}_3) = 0.011 \text{ s}^{-1}$ for August 21 case. Similar analyses were performed for 11 additional cases during the campaign, and the derived results are summarized in Table 2. The determined γ values range from 0.021 to 0.102, with a mean value of 15 0.061 ± 0.025 . The average $k(\text{NO}_3)$ derived from the steady state fits is $0.015 \pm 0.010 \text{ s}^{-1}$, which is comparable to that predicted from the VOC measurements described above. The agreement between these two methods also corroborates the determination of the uptake coefficient from steady state analysis.

Compared with the previous field-determined N_2O_5 uptake coefficients (0.002-0.04) from aircraft, tower, and mountaintop measurements in the USA and southern China (e.g., Brown et al., 2006; Morgan et al., 2015; Brown et al., 2016), the observed 20 γ values in the present study are significantly higher. The large variability of γ at Mt. Tai is similar to that observed at a rural high-elevation site in Germany and obtained from other ambient measurement derivations (Wagner et al., 2013; Phillips et al., 2016). A recent laboratory study has reported high γ (> 0.05) of isotope-labeled N_2O_5 into aqueous nitrate-containing aerosols and largely enhancement of uptake at higher RH conditions (Gržinić et al., 2016), which help rationalize our field results with larger uptake coefficient than many previous studies. Moreover, a measurement at an urban surface site in Jinan close to Mt. 25 Tai gave similarly high values of γ (0.042-0.092) (Wang et al., 2017b). This may suggest a unique feature of the reactive nitrogen chemistry with rapid heterogeneous N_2O_5 loss over this region, and is consistent with the observed low N_2O_5 levels but relatively high ClNO_2 and particulate nitrate produced from the heterogeneous reactions.

Previous laboratory studies have investigated the dependence of γ on aerosol compositions, and have developed mechanistic parameterizations of γ that can be employed in air quality models (Chang et al., 2011 and references therein). A commonly 30 used parameterization was proposed by Bertram and Thornton (2009) and considered the aerosol volume-to-surface ratio (V/S), concentrations of nitrate, chloride, and water. For comparison, γ values were calculated using this parameterization based on



the measured aerosol composition and molarity of water determined from the E-AIM model (<http://www.aim.env.uea.ac.uk/aim/model4/model4a.php>) (Wexler and Clegg, 2002). In the calculation, mean values of V/S (64.8 - 77.2 nm) measured in the present study instead of empirical pre-factor A were used, and the reaction rate coefficients were employed as the empirical values suggested by Bertram and Thornton (2009).

5 Figure 8 shows a comparison of the γ values determined from parameterization and measurements. Overall, the parameterized γ shows good correlation ($r = 0.87$) with the observation determined values, and gives an average of 0.063 ± 0.006 , which is in good agreement with the average of 0.061 ± 0.025 derived from steady state analysis. However, the γ values from BT-parameterization are in the range of 0.052-0.070, with much lower variability than the measurement determined values. Similar results with compatible averaged γ values between measurements and parameterization predictions but higher variability for
10 measurement derived γ have been reported at a mountain measurement in Germany (Phillips et al., 2016). A distinct difference of γ between the steady-state analysis and the parameterization has also been reported by Chang et al., (2016), who suggested that the uncertainty in determining aerosol water content would introduce errors in the parameterization. Bertram and Thornton (2009) suggested that predicted γ values would plateau and be independent of particulate chemical composition at particle water molarity above 15M. In the present study, the particle water molarity in these cases was consistently above 25 M because
15 of the high RH and frequent cloud cover at the mountain site, which may explain the lower variability of γ values predicted by parameterization.

A moderate negative dependence ($r = 0.50$) of determined γ on aerosol nitrate concentration can be inferred, with lower values of γ associated with higher nitrate content (cf. Figure S1). This is consistent with the anti-correlation of γ and nitrate from tower measurements in the USA and aircraft measurements over the UK (Wagner et al., 2013; Morgan et al., 2015), and
20 consistent with most of the parameterizations reviewed by Chang et al. (2011). Nevertheless, the moderate correlation observed here may result from the complicated relationship between nitrate and N_2O_5 uptake. Under certain conditions, nitrate can suppress the N_2O_5 uptake (Bertram and Thornton, 2009); but meanwhile, particulate nitrate is a product of N_2O_5 hydrolysis, and thus efficient uptake may be accompanied by higher nitrate concentrations (Phillips et al., 2016). It is very difficult to differentiate nitrate produced in situ from preexisting nitrate; therefore, covariation and suppression effects may disguise the
25 relationship between γ and nitrate.

Furthermore, as suggested by Bertram and Thornton (2009), the presence of chloride can offset the suppression of N_2O_5 uptake by nitrate. The determined γ in the present study also show positive dependence on aerosol chloride concentration ($r = 0.61$), indicating the enhancement of N_2O_5 uptake by increased chloride contents in aerosols. This can be better described by the clear positive dependence ($r = 0.84$) of γ on the molar ratio of particulate chloride to nitrate, as illustrated by the color-coded data
30 in Figure 8. The variation in γ values determined in the present study appears to be controlled largely by the particulate chloride-to-nitrate ratio, broadly following the competing effects of nitrate and chloride in the parameterization (Bertram and Thornton, 2009; Ryder et al., 2014). However, the discrepancy between the measurement- and parameterization-derived values may imply that some mechanisms and factors affecting γ under conditions of high humid and pollution (e.g., reacto-diffusive length,



salting effects, etc.) (Gaston and Thornton, 2016; Gržinić et al., 2016) should be further explicitly considered in the parameterization. The in situ $\gamma_{\text{N}_2\text{O}_5}$ measurement technique developed by Bertram et al. (2009a) may be useful in directly investigating the complex dependence of γ on different factors in a range of environments.

3.4 ClNO₂ production yield

- 5 To characterize the formation of ClNO₂ from rapid heterogeneous N₂O₅ uptake and sufficient particulate chloride, the yields of ClNO₂ (ϕ) were examined for different plumes. The ϕ defined in R3 can be estimated from the ratio between ClNO₂ production rate and N₂O₅ loss rate:

$$\phi = \frac{\Delta \text{ClNO}_2}{\Delta \text{N}_2\text{O}_5} = \frac{d\text{ClNO}_2/dt}{d\text{N}_2\text{O}_5/dt} = \frac{d\text{ClNO}_2/dt}{k(\text{N}_2\text{O}_5)_{\text{het}}[\text{N}_2\text{O}_5]} = \frac{[\text{ClNO}_2]}{\int k(\text{N}_2\text{O}_5)_{\text{het}}[\text{N}_2\text{O}_5] dt} \quad (6)$$

10 $k(\text{N}_2\text{O}_5)$ values can be determined using the inverse steady-state lifetime analysis described above, and the production rate of ClNO₂ can be derived from the near-linear increase in ClNO₂ mixing ratio observed during a period of roughly constant composition and environmental variables. For the intercepted power plant plumes exhibiting sharp ClNO₂ peaks, the ClNO₂ yield can be estimated from the ratio of the observed ClNO₂ mixing ratio to the integrated N₂O₅ uptake loss. This analysis assumes that no ClNO₂ was present at the point of plume emission from the sources and no ClNO₂ formation before sunset, and that the γ within the power plant plumes did not change during the transport from the source to the measurement site.

15 Two examples of the analysis are shown in Figure 9, which indicate the time periods in which ClNO₂ concentration increased while other parameters (such as N₂O₅, NO_x, O₃, and SO₂ concentrations) were relatively stable. The ϕ values obtained for these two cases were 0.26 and 0.05 for July 27 and August 6, respectively. Similar analyses were performed for all of other selected cases in which the ClNO₂ concentration increased and other relevant parameters were relatively constant for a short period, typically 1-3 h, and the obtained results were summarized in Table 2. The determined ϕ for the seven power plant plumes are
20 also listed in Table 1. During the measurement period, ϕ varied from 0.02 to 0.90, with an average of 0.27 ± 0.24 and a median of 0.20. The large variability of ϕ is similar to field-derived values in most previous studies, and the mean value is comparable to that in the nocturnal residual layer over continental Colorado (0.18) (Thornton et al., 2010), but lower than that observed at a mountain site in Germany (0.49) (Phillips et al., 2016). The ϕ values for the power plant plumes (range of 0.20-0.90; average: 0.46 ± 0.24) are generally higher than the campaign average and those from regional diffuse pollution cases. The maximum ϕ
25 (0.90) corresponds to the plume with the highest ClNO₂ mixing ratio observed during the campaign. This is consistent with a tower measurement in Colorado, in which higher ClNO₂ yields were also observed in inland power plant plumes (Riedel et al., 2013).

Similar to that developed for γ , a parameterization of ClNO₂ yield as a function of aerosol water and chlorine composition has been proposed based on laboratory studies (Bertram and Thornton, 2009; Roberts et al., 2009):

$$\phi = \frac{[\text{Cl}^-]}{k'[\text{H}_2\text{O}] + [\text{Cl}^-]} \quad (7)$$



We compared the field-derived values to the parameterization for cases with available aerosol compositions, using an empirical k' of 450, as recommended by Roberts et al. (2009). As shown in Figure 10a, the ϕ values predicted by the parameterization are generally higher than those determined from observed ClNO₂ production rates, especially at low measurement-determined yields. For measured ϕ values higher than 0.4, smaller differences (<20%) were observed between the two methods, which are within the aggregate uncertainty associated with measurement and derivation. The parameterized ϕ values exhibit positive dependence on the aerosol chloride concentration and the Cl/H₂O ratio. The measurement-determined values only exhibit measurable such dependence at low yields, implying the possible biased relationship due to higher aerosol water conditions in the present work. The discrepancy between the parameterization ϕ based upon aerosol composition and those derived from measured ClNO₂ concentrations has been found previously (e.g., Wagner et al., 2013), and the underlying causes have not been resolved.

By examining the relationships between the determined yield and other parameters, we found a slightly negative relationship between ϕ and particulate nitrate concentration, as depicted in Figure 10b. Although the data are scattered, the high-yield cases are mostly associated with lower nitrate concentrations, while the ϕ for the high nitrate cases (>15 $\mu\text{g m}^{-3}$) are smaller. A similar trend was observed for the NO_x/NO_y ratio, which indicates the ‘age’ of the air masses, suggesting that higher ϕ are usually associated with relatively ‘young’ air masses exhibiting low nitrate concentrations. More secondary and dissolved organic matters in aged aerosols could be a possible factor contributing to the reduction of ClNO₂ production efficiency (Mielke et al., 2013; Ryder et al., 2015; Phillips et al., 2016). Further studies are needed to characterize the combined effects of various parameters on ClNO₂ yields, in particular the influences of the aerosol mixing state, chloride availability distribution among particle sizes, organic matter, acidity, other possible loss ways of ClNO₂, and potential factors affecting in high humid and polluted conditions (Laskin et al., 2012; Mielke et al., 2013; Wagner et al., 2013; Ryder et al., 2015; Li et al., 2016; Phillips et al., 2016).

3.5 Effects of heterogeneous N₂O₅ reactions on nitrate formation and NO_x processing

In addition to abundant ClNO₂ formation, rapid heterogeneous N₂O₅ uptake may also lead to the production of a large amount of nitrate, which is one of the main components of fine particles contributing to haze pollution in northern China (e.g., Huang et al., 2014). Based on the reactions described above, the formation rate of soluble nitrate $p(\text{NO}_3^-)$ can be determined from the ClNO₂ yield and N₂O₅ heterogeneous loss rate as follows:

$$p(\text{NO}_3^-) = (2 - \phi) \frac{d[\text{N}_2\text{O}_5]}{dt} = (2 - \phi) k_{\text{N}_2\text{O}_5} [\text{N}_2\text{O}_5] \quad (8)$$

The $p(\text{NO}_3^-)$ values obtained for the select cases during the study period ranged from 0.02 to 0.62 ppt s⁻¹, with a mean value of 0.29 ± 0.18 ppt s⁻¹, corresponding to 0.2- 4.8 $\mu\text{g m}^{-3} \text{ hr}^{-1}$ and 2.2 ± 1.4 $\mu\text{g m}^{-3} \text{ hr}^{-1}$ (Table 2). The derived rates are comparable to the observed increases in nitrate concentrations (2-5 $\mu\text{g m}^{-3} \text{ h}^{-1}$) during haze episodes in summer nights at a rural site in the NCP (Wen et al., 2015). The NO₃⁻ formation was predicted by integrating each derived formation rate over the corresponding



analysis period. For power plant plumes, we equated the measured nitrate concentrations with the increases by assuming that no aerosol nitrate was directly emitted from the nocturnal point sources. As shown in Figure 11, the predicted nitrate formation shows reasonable agreement with the measured increases in nitrate concentrations (ΔNO_3^-) (RMA slope of 1.14 and $r = 0.81$). This consistency also can serve as a check for the reliability of the above determined heterogeneous N_2O_5 reactivity. The in-situ nitrate formation from heterogeneous N_2O_5 reactions was predicted to be as high as $17 \mu\text{g m}^{-3}$, with a mean value of $4.3 \pm 4.5 \mu\text{g m}^{-3}$, accounting for $32 (\pm 27) \%$ of the observed average nitrate concentration during the cases. This is consistent with the maximum nitrate increase of $14.9 \mu\text{g m}^{-3}$ over south China (Li et al., 2016) and 21% nitrate increase in polluted episodes in Beijing (Su et al., 2017) after considering the heterogeneous N_2O_5 uptake in the regional model simulation. As for a plume undergo continuous chemical processing from dusk to sunrise, the heterogeneous N_2O_5 reactions would lead to substantial nitrate formation (e.g., $22 \mu\text{g m}^{-3}$ production for a 10-h night), and could contribute significantly to secondary fine aerosols as the main driver of the persistent haze pollution in northern China.

The formation of nitrate (including HNO_3) and its subsequent removal by deposition is the predominant removal mechanism of nitrogen oxides from the atmosphere (Chang et al., 2011). The nocturnal NO_x removal rate depends on the NO_3 radical production rate, heterogeneous N_2O_5 loss rate, NO_3 reaction rate with VOCs, the partitioning between N_2O_5 and NO_3 concentrations, and ClNO_2 yield. ClNO_2 mainly functions as a reservoir of NO_x , rather than as a sink, because the formation of ClNO_2 throughout the night with subsequent morning photolysis recycles NO_2 (Wang et al., 2016). For simplicity, the reactions of NO_3 with VOCs can be assumed to result in the complete removal of reactive nitrogen (Wagner et al., 2013), and this assumption does not significantly affect results because the loss of NO_3 with VOCs accounts for less than 30% of the total N_2O_5 reactivity. Thus, the nocturnal NO_x loss rate can be quantified by the following equation:

$$L(\text{NO}_x) = (2 - \phi)k_{\text{N}_2\text{O}_5}[\text{N}_2\text{O}_5] + k_{\text{NO}_3}[\text{NO}_3] = (1 - \phi)k_{\text{N}_2\text{O}_5}[\text{N}_2\text{O}_5] + p[\text{NO}_3] \quad (9)$$

Using the coefficients described above, we calculated the nocturnal loss rate of NO_x for each case, as summarized in Table 2. The NO_x removal rate varied from 0.19 to 2.34 ppb h^{-1} , with a mean of $1.12 \pm 0.63 \text{ ppb h}^{-1}$. This loss rate is higher than that determined from tower measurements during wintertime in Colorado, with integrated nocturnal NO_2 loss ranging from 2.2 to 4.4 ppbv (Wagner et al., 2013). Figure 12 shows the relationship between determined NO_x loss rate and observed ambient NO_x concentration at the measurement site. NO_x loss rate appears to be strongly dependent upon NO_x concentrations below 6 pptv (slope = 0.32 h^{-1} ; $r = 0.93$); the loss rate became more scattered at higher NO_x conditions, which were typically observed in the power plant plumes. This result implies that for low NO_x condition ($<6 \text{ ppbv}$), 96% of NO_x would be removed after 3-h of nocturnal processing, if no additional NO_x emissions affect the plume during this period.

Comparing NO_x loss to the nitrate formation rates, it can be inferred that the nitrate formation from heterogeneous N_2O_5 uptake is predominant in reactive NO_x loss and account for an average of 87% of the NO_x loss, although this fraction of individual cases varied between 35 to 100%. A box model simulation based on tower measurements at Colorado also reported that the largest proportion of the nitrate radical chemistry is N_2O_5 hydrolysis, which typically accounted for 80% of nitrate radical



production, whereas the losses to NO_3 -VOC reactions are less than 10% (Wagner et al., 2013). A recent model simulation for southern China also suggested that considering the N_2O_5 uptake and subsequent Cl activation could decrease regional NO_x by more than 16% (Li et al., 2016). The results obtained in the present study demonstrate the significance of fast heterogeneous N_2O_5 chemistry on nocturnal NO_x removal and fine nitrate formation in the polluted residual layer over the NCP.

5 4. Summary and Conclusions

An intensive field study was conducted at a high-altitude site to characterize the reactive nitrogen chemistry in the polluted nocturnal residual layer over the NCP. The results revealed the frequently elevated ClNO_2 mixing ratios (maximum: 2065 pptv) and efficient ClNO_2 yields (0.46 ± 0.24) resulting from power plant plumes in the residual layer. The presence of ClNO_2 -laden air in the nocturnal residual layer confirms our previous hypothesis based on a measurement in a rural site in the NCP, that the downward mixing of ClNO_2 -rich air to the surface in the next morning would have large impacts on early morning photochemistry and ozone production. Rapid heterogeneous N_2O_5 uptake and efficient ClNO_2 and nitrate formation were observed during the study period. The γ determined in the present study (average: 0.061 ± 0.025) exhibited a clear dependence on the particulate chloride-to-nitrate ratio, and are higher than those observed in other locations, but consistent with those obtained at a surface site in the same region of the NCP. Laboratory-derived parameterizations predicted comparable mean γ values, but did not represent the high variability of the measured values, and tended to overestimate ϕ in the low yields. These discrepancies suggest that various aerosol physicochemical parameters have complicated effects on N_2O_5 uptake and ClNO_2 yield, in particular in high humid and polluted residual layer, which requires further investigation.

Fast heterogeneous N_2O_5 uptake dominated the regional nocturnal NO_x loss, resulting in a mean loss rate of 1.12 ± 0.63 ppb h^{-1} and accounting for an average of 87% of the nocturnal NO_x loss. Moreover, heterogeneous reactions contributed to substantial nitrate production up to $17 \mu\text{g m}^{-3}$, with a mean nocturnal formation rate of $2.2 \pm 1.4 \mu\text{g m}^{-3} \text{hr}^{-1}$, which may help explain the previously observed rapid nighttime growth of fine nitrate aerosols in the NCP. The results demonstrate the significance of heterogeneous N_2O_5 - ClNO_2 chemistry in the polluted residual layer over the NCP, which underpins the need for further studies regarding their roles in the formation of complex haze pollution in northern China.

Acknowledgments.

The authors would like to thank Dr. Fu Xiao for help in providing the location information of power plants in Shandong. HYSPLIT model is made available by the NOAA Air Resources Laboratory. This work was funded by the National Natural Science Foundation of China (91544213, 41505103, 41275123) and the PolyU Project of Strategic Importance (1-ZE13). The authors also acknowledge the support of the Research Institute for Sustainable Urban Development (RISUD).



References

- Abbatt, J., Lee, A., and Thornton, J.: Quantifying trace gas uptake to tropospheric aerosol: recent advances and remaining challenges, *Chem. Soc. Rev.*, 41, 6555-6581, 2012.
- 5 Ammann, M., Cox, R. A., Crowley, J. N., Jenkin, M. E., Mellouki, A., Rossi, M. J., Troe, J., and Wallington, T. J.: Evaluated kinetic and photochemical data for atmospheric chemistry: Volume VI – heterogeneous reactions with liquid substrates, *Atmos. Chem. Phys.*, 13, 8045-8228, 2013.
- Anttila, T., Kiendler-Scharr, A., Tillmann, R., and Mentel, T. F.: On the Reactive Uptake of Gaseous Compounds by Organic-Coated Aqueous Aerosols: Theoretical Analysis and Application to the Heterogeneous Hydrolysis of N₂O₅, *J. Phys. Chem. A*, 110, 10435-10443, 2006.
- 10 Atkinson, R., and Arey, J.: Atmospheric Degradation of Volatile Organic Compounds, *Chem. Rev.*, 103, 4605-4638, 2003.
- Bertram, T. H., and Thornton, J. A.: Toward a general parameterization of N₂O₅ reactivity on aqueous particles: the competing effects of particle liquid water, nitrate and chloride, *Atmos. Chem. Phys.*, 9, 8351-8363, 2009.
- Bertram, T. H., Thornton, J. A., and Riedel, T. P.: An experimental technique for the direct measurement of N₂O₅ reactivity on ambient particles, *Atmos. Meas. Tech.*, 2, 231-242, 2009a.
- 15 Bertram, T. H., Thornton, J. A., Riedel, T. P., Middlebrook, A. M., Bahreini, R., Bates, T. S., Quinn, P. K., and Coffman, D. J.: Direct observations of N₂O₅ reactivity on ambient aerosol particles, *Geophys. Res. Lett.*, 36, 10.1029/2009GL040248, 2009b.
- Brown, S., Ryerson, T., Wollny, A., Brock, C., Peltier, R., Sullivan, A., Weber, R., Dube, W., Trainer, M., and Meagher, J.: Variability in nocturnal nitrogen oxide processing and its role in regional air quality, *Science*, 311, 67-70, 2006.
- 20 Brown, S. S., Dubé, W. P., Osthoff, H. D., Stutz, J., Ryerson, T. B., Wollny, A. G., Brock, C. A., Warneke, C., de Gouw, J. A., Atlas, E., Neuman, J. A., Holloway, J. S., Lerner, B. M., Williams, E. J., Kuster, W. C., Goldan, P. D., Angevine, W. M., Trainer, M., Fehsenfeld, F. C., and Ravishankara, A. R.: Vertical profiles in NO₃ and N₂O₅ measured from an aircraft: Results from the NOAA P-3 and surface platforms during the New England Air Quality Study 2004, *J. Geophys. Res. -Atmos.*, 112, 10.1029/2007JD008883, 2007.
- 25 Brown, S. S., Dubé, W. P., Fuchs, H., Ryerson, T. B., Wollny, A. G., Bahreini, R., Middlebrook, A. M., Neuman, J. A., Atlas, E., Roberts, J. M., Osthoff, H. D., Trainer, M., Fehsenfeld, F. C., and Ravishankara, A. R.: Reactive uptake coefficients for N₂O₅ determined from aircraft measurements during the Second Texas Air Quality Study: Comparison to current model parameterizations, *J. Geophys. Res. -Atmos.*, 114, 10.1029/2008JD011679, 2009.
- Brown, S. S., Dubé, W. P., Tham, Y. J., Zha, Q., Xue, L., Poon, S., Wang, Z., Blake, D. R., Tsui, W., Parrish, D. D., and Wang, T.: Nighttime Chemistry at a High Altitude Site Above Hong Kong, *J. Geophys. Res. -Atmos.*, 10.1002/2015jd024566, 10.1002/2015jd024566, 2016.
- 30 Chang, W. L., Bhave, P. V., Brown, S. S., Riemer, N., Stutz, J., and Dabdub, D.: Heterogeneous Atmospheric Chemistry, Ambient Measurements, and Model Calculations of N₂O₅: A Review, *Aerosol Sci. Technol.*, 45, 665-695, 10.1080/02786826.2010.551672, 2011.
- 35 Chang, W. L., Brown, S. S., Stutz, J., Middlebrook, A. M., Bahreini, R., Wagner, N. L., Dubé, W. P., Pollack, I. B., Ryerson, T. B., and Riemer, N.: Evaluating N₂O₅ heterogeneous hydrolysis parameterizations for CalNex 2010, *J. Geophys. Res. -Atmos.*, 121, 5051-5070, 10.1002/2015JD024737, 2016.
- Davis, J. M., Bhave, P. V., and Foley, K. M.: Parameterization of N₂O₅ reaction probabilities on the surface of particles containing ammonium, sulfate, and nitrate, *Atmos. Chem. Phys.*, 8, 5295-5311, 10.5194/acp-8-5295-2008, 2008.
- 40 Draxler, R. R., and Hess, G. D.: An overview of the HYSPLIT_4 modelling system for trajectories, dispersion and deposition, *Aust. Meteorol. Mag.*, 47, 295-308, 1998.
- Evans, M. J., and Jacob, D. J.: Impact of new laboratory studies of N₂O₅ hydrolysis on global model budgets of tropospheric nitrogen oxides, ozone, and OH, *Geophys. Res. Lett.*, 32, 10.1029/2005GL022469, 2005.
- Faxon, C., Bean, J., and Ruiz, L.: Inland Concentrations of Cl₂ and ClNO₂ in Southeast Texas Suggest Chlorine Chemistry Significantly Contributes to Atmospheric Reactivity, *Atmosphere*, 6, 1487, 2015.
- 45 Finlayson-Pitts, B. J., Ezell, M. J., and Pitts, J. N.: Formation of chemically active chlorine compounds by reactions of atmospheric NaCl particles with gaseous N₂O₅ and ClONO₂, *Nature*, 337, 241-244, 1989.



- Foley, K. M., Roselle, S. J., Appel, K. W., Bhave, P. V., Pleim, J. E., Otte, T. L., Mathur, R., Sarwar, G., Young, J. O., Gilliam, R. C., Nolte, C. G., Kelly, J. T., Gilliland, A. B., and Bash, J. O.: Incremental testing of the Community Multiscale Air Quality (CMAQ) modeling system version 4.7, *Geosci. Model Dev.*, 3, 205-226, 2010.
- 5 Gao, J., Wang, T., Ding, A., and Liu, C.: Observational study of ozone and carbon monoxide at the summit of mount Tai (1534m a.s.l.) in central-eastern China, *Atmos. Environ.*, 39, 4779-4791, 2005.
- Gaston, C. J., and Thornton, J. A.: Reacto-Diffusive Length of N₂O₅ in Aqueous Sulfate- and Chloride-Containing Aerosol Particles, *J. Phys. Chem. A*, 120, 1039-1045, 2016.
- Griffiths, P. T., Badger, C. L., Cox, R. A., Folkers, M., Henk, H. H., and Mentel, T. F.: Reactive Uptake of N₂O₅ by Aerosols Containing Dicarboxylic Acids. Effect of Particle Phase, Composition, and Nitrate Content, *J. Phys. Chem. A*, 113, 5082-5090, 2009.
- 10 Gržinić, G., Bartels-Rausch, T., Türler, A., and Ammann, M.: Efficient bulk mass accommodation of N₂O₅ into neutral aqueous aerosol, *Atmos. Chem. Phys. Discuss.*, 2016, 1-13, 10.5194/acp-2016-1118, 2016.
- Guo, J., Wang, Y., Shen, X., Wang, Z., Lee, T., Wang, X., Li, P., Sun, M., Collett, J., Wang, W., and Wang, T.: Characterization of cloud water chemistry at Mount Tai, China: Seasonal variation, anthropogenic impact, and cloud processing, *Atmos. Environ.*, 60, 2012.
- 15 Huang, R.-J., Zhang, Y., Bozzetti, C., Ho, K.-F., Cao, J.-J., Han, Y., Daellenbach, K. R., Slowik, J. G., Platt, S. M., Canonaco, F., Zotter, P., Wolf, R., Pieber, S. M., Brunns, E. A., Crippa, M., Ciarelli, G., Piazzalunga, A., Schwikowski, M., Abbaszade, G., Schnelle-Kreis, J., Zimmermann, R., An, Z., Szidat, S., Baltensperger, U., Haddad, I. E., and Prevot, A. S. H.: High secondary aerosol contribution to particulate pollution during haze events in China, *Nature*, 514, 218-222, 2014.
- 20 Laskin, A., Moffet, R. C., Gilles, M. K., Fast, J. D., Zaveri, R. A., Wang, B., Nigge, P., and Shutthanandan, J.: Tropospheric chemistry of internally mixed sea salt and organic particles: Surprising reactivity of NaCl with weak organic acids, *J. Geophys. Res. -Atmos.*, 117, 10.1029/2012JD017743, 2012.
- Li, Q., Zhang, L., Wang, T., Tham, Y. J., Ahmadov, R., Xue, L., Zhang, Q., and Zheng, J.: Impacts of heterogeneous uptake of dinitrogen pentoxide and chlorine activation on ozone and reactive nitrogen partitioning: improvement and application of the WRF-Chem model in southern China, *Atmos. Chem. Phys.*, 16, 14875-14890, 2016.
- 25 Ma, N., Zhao, C., Tao, J., Wu, Z., Kecorius, S., Wang, Z., Groß, J., Liu, H., Bian, Y., Kuang, Y., Teich, M., Spindler, G., Müller, K., van Pinxteren, D., Herrmann, H., Hu, M., and Wiedensohler, A.: Variation of CCN activity during new particle formation events in the North China Plain, *Atmos. Chem. Phys.*, 16, 8593-8607, 2016.
- 30 Mielke, L. H., Furgeson, A., and Osthoff, H. D.: Observation of ClNO₂ in a Mid-Continental Urban Environment, *Environ. Sci. Technol.*, 45, 8889-8896, 2011.
- Mielke, L. H., Stutz, J., Tsai, C., Hurlock, S. C., Roberts, J. M., Veres, P. R., Froyd, K. D., Hayes, P. L., Cubison, M. J., Jimenez, J. L., Washenfelder, R. A., Young, C. J., Gilman, J. B., de Gouw, J. A., Flynn, J. H., Grossberg, N., Lefer, B. L., Liu, J., Weber, R. J., and Osthoff, H. D.: Heterogeneous formation of nitryl chloride and its role as a nocturnal NO_x reservoir species during CalNex-LA 2010, *J. Geophys. Res. -Atmos.*, 118, 10638-10652, 2013.
- 35 Morgan, W., Ouyang, B., Allan, J., Aruffo, E., Di Carlo, P., Kennedy, O., Lowe, D., Flynn, M., Rosenberg, P., and Williams, P.: Influence of aerosol chemical composition on N₂O₅ uptake: airborne regional measurements in northwestern Europe, *Atmos. Chem. Phys.*, 15, 973-990, 2015.
- Osthoff, H. D., Roberts, J. M., Ravishankara, A. R., Williams, E. J., Lerner, B. M., Sommariva, R., Bates, T. S., Coffman, D., Quinn, P. K., Dibb, J. E., Stark, H., Burkholder, J. B., Talukdar, R. K., Meagher, J., Fehsenfeld, F. C., and Brown, S. S.: High levels of nitryl chloride in the polluted subtropical marine boundary layer, *Nat. Geosci.*, 1, 324-328, 2008.
- 40 Pathak, R. K., Wu, W. S., and Wang, T.: Summertime PM_{2.5} ionic species in four major cities of China: nitrate formation in an ammonia-deficient atmosphere, *Atmos. Chem. Phys.*, 9, 1711-1722, 2009.
- Pathak, R. K., Wang, T., and Wu, W. S.: Nighttime enhancement of PM_{2.5} nitrate in ammonia-poor atmospheric conditions in Beijing and Shanghai: Plausible contributions of heterogeneous hydrolysis of N₂O₅ and HNO₃ partitioning, *Atmos. Environ.*, 45, 1183-1191, 2011.
- 45 Phillips, G. J., Tang, M. J., Thieser, J., Brickwedde, B., Schuster, G., Bohn, B., Lelieveld, J., and Crowley, J. N.: Significant concentrations of nitryl chloride observed in rural continental Europe associated with the influence of sea salt chloride and anthropogenic emissions, *Geophys. Res. Lett.*, 39, 10.1029/2012GL051912, 2012.



- Phillips, G. J., Thieser, J., Tang, M., Sobanski, N., Schuster, G., Fachinger, J., Drewnick, F., Borrmann, S., Bingemer, H., Lelieveld, J., and Crowley, J. N.: Estimating N₂O₅ uptake coefficients using ambient measurements of NO₃, N₂O₅, ClNO₂ and particle-phase nitrate, *Atmos. Chem. Phys.*, 16, 13231-13249, 2016.
- 5 Riedel, T. P., Bertram, T. H., Crisp, T. A., Williams, E. J., Lerner, B. M., Vlasenko, A., Li, S. M., Gilman, J., de Gouw, J., Bon, D. M., Wagner, N. L., Brown, S. S., and Thornton, J. A.: Nitryl Chloride and Molecular Chlorine in the Coastal Marine Boundary Layer, *Environ. Sci. Technol.*, 46, 10463-10470, 2012.
- Riedel, T. P., Wagner, N. L., Dubé, W. P., Middlebrook, A. M., Young, C. J., Öztürk, F., Bahreini, R., VandenBoer, T. C., Wolfe, D. E., Williams, E. J., Roberts, J. M., Brown, S. S., and Thornton, J. A.: Chlorine activation within urban or power plant plumes: Vertically resolved ClNO₂ and Cl₂ measurements from a tall tower in a polluted continental setting, *J. Geophys. Res. -Atmos.*, 118, 8702-8715, 10.1002/jgrd.50637, 2013.
- 10 Riemer, N., Vogel, H., Vogel, B., Anttila, T., Kiendler-Scharr, A., and Mentel, T. F.: Relative importance of organic coatings for the heterogeneous hydrolysis of N₂O₅ during summer in Europe, *J. Geophys. Res. -Atmos.*, 114, 10.1029/2008JD011369, 2009.
- Roberts, J. M., Osthoff, H. D., Brown, S. S., Ravishankara, A. R., Coffman, D., Quinn, P., and Bates, T.: Laboratory studies of products of N₂O₅ uptake on Cl⁻ containing substrates, *Geophys. Res. Lett.*, 36, 10.1029/2009gl040448, 2009.
- 15 Ryder, O. S., Ault, A. P., Cahill, J. F., Guasco, T. L., Riedel, T. P., Cuadra-Rodriguez, L. A., Gaston, C. J., Fitzgerald, E., Lee, C., Prather, K. A., and Bertram, T. H.: On the Role of Particle Inorganic Mixing State in the Reactive Uptake of N₂O₅ to Ambient Aerosol Particles, *Environ. Sci. Technol.*, 48, 1618-1627, 10.1021/es4042622, 2014.
- Ryder, O. S., Campbell, N. R., Shalowski, M., Al-Mashat, H., Nathanson, G. M., and Bertram, T. H.: Role of Organics in Regulating ClNO₂ Production at the Air–Sea Interface, *J. Phys. Chem. A*, 119, 8519-8526, 2015.
- 20 Simon, H., Kimura, Y., McGaughey, G., Allen, D. T., Brown, S. S., Osthoff, H. D., Roberts, J. M., Byun, D., and Lee, D.: Modeling the impact of ClNO₂ on ozone formation in the Houston area, *J. Geophys. Res. -Atmos.*, 114, 10.1029/2008JD010732, 2009.
- Simpson, W. R., Brown, S. S., Saiz-Lopez, A., Thornton, J. A., and Glasow, R. v.: Tropospheric Halogen Chemistry: Sources, Cycling, and Impacts, *Chem. Rev.*, 10.1021/cr5006638, 10.1021/cr5006638, 2015.
- 25 Su, X., Tie, X., Li, G., Cao, J., Huang, R., Feng, T., Long, X., and Xu, R.: Effect of hydrolysis of N₂O₅ on nitrate and ammonium formation in Beijing China: WRF-Chem model simulation, *Sci. Total Environ.*, 579, 221-229, 2017.
- Sun, L., Xue, L., Wang, T., Gao, J., Ding, A., Cooper, O. R., Lin, M., Xu, P., Wang, Z., Wang, X., Wen, L., Zhu, Y., Chen, T., Yang, L., Wang, Y., Chen, J., and Wang, W.: Significant increase of summertime ozone at Mount Tai in Central Eastern China, *Atmos. Chem. Phys.*, 16, 10637-10650, 2016.
- 30 Tang, M. J., Telford, P. J., Pope, F. D., Rkiouak, L., Abraham, N. L., Archibald, A. T., Braesicke, P., Pyle, J. A., McGregor, J., Watson, I. M., Cox, R. A., and Kalberer, M.: Heterogeneous reaction of N₂O₅ with airborne TiO₂ particles and its implication for stratospheric particle injection, *Atmos. Chem. Phys.*, 14, 6035-6048, 2014.
- Tham, Y. J., Wang, Z., Li, Q., Yun, H., Wang, W., Wang, X., Xue, L., Lu, K., Ma, N., Bohn, B., Li, X., Kecorius, S., Größ, J., Shao, M., Wiedensohler, A., Zhang, Y., and Wang, T.: Significant concentrations of nitryl chloride sustained in the morning: Investigations of the causes and impacts on ozone production in a polluted region of northern China, *Atmos. Chem. Phys.*, 16, 14959-14977, 2016.
- 35 Thornton, J. A., Kercher, J. P., Riedel, T. P., Wagner, N. L., Cozic, J., Holloway, J. S., Dubé, W. P., Wolfe, G. M., Quinn, P. K., Middlebrook, A. M., Alexander, B., and Brown, S. S.: A large atomic chlorine source inferred from mid-continental reactive nitrogen chemistry, *Nature*, 464, 271-274, 2010.
- 40 Wagner, N. L., Riedel, T. P., Young, C. J., Bahreini, R., Brock, C. A., Dubé, W. P., Kim, S., Middlebrook, A. M., Öztürk, F., Roberts, J. M., Russo, R., Sive, B., Swarthout, R., Thornton, J. A., VandenBoer, T. C., Zhou, Y., and Brown, S. S.: N₂O₅ uptake coefficients and nocturnal NO₂ removal rates determined from ambient wintertime measurements, *J. Geophys. Res. -Atmos.*, 118, 9331-9350, 10.1002/jgrd.50653, 2013.
- 45 Wang, T., Ding, A. J., Gao, J., and Wu, W. S.: Strong ozone production in urban plumes from Beijing, China, *Geophys. Res. Lett.*, 33, 10.1029/2006gl027689, 2006.
- Wang, T., Tham, Y. J., Xue, L., Li, Q., Zha, Q., Wang, Z., Poon, S. C. N., Dubé, W. P., Blake, D. R., Louie, P. K. K., Luk, C. W. Y., Tsui, W., and Brown, S. S.: Observations of nitryl chloride and modeling its source and effect on ozone in the planetary boundary layer of southern China, *J. Geophys. Res. -Atmos.*, 10.1002/2015jd024556, 10.1002/2015jd024556, 2016.
- 50



- Wang, T., Xue, L., Brimblecombe, P., Lam, Y. F., Li, L., and Zhang, L.: Ozone pollution in China: A review of concentrations, meteorological influences, chemical precursors, and effects, *Sci. Total. Environ.*, 575, 1582-1596, 2017a.
- Wang, X., Wang, H., Xue, L., Wang, T., Wang, L., Gu, R., Wang, W., Tham, Y. J., Wang, Z., Yang, L., Chen, J., and Wang, W.: Observations of N₂O₅ and ClNO₂ at a polluted urban surface site in North China: High N₂O₅ uptake coefficients and low ClNO₂ product yields, *Atmos. Environ.*, 156, 125-134, 2017b.
- 5 Wang, Z., Wang, T., Gao, R., Xue, L., Guo, J., Zhou, Y., Nie, W., Wang, X., Xu, P., Gao, J., Zhou, X., Wang, W., and Zhang, Q.: Source and variation of carbonaceous aerosols at Mount Tai, North China: Results from a semi-continuous instrument, *Atmos. Environ.*, 45, 1655-1667, 2011.
- 10 Wen, L., Chen, J., Yang, L., Wang, X., Caihong, X., Sui, X., Yao, L., Zhu, Y., Zhang, J., Zhu, T., and Wang, W.: Enhanced formation of fine particulate nitrate at a rural site on the North China Plain in summer: The important roles of ammonia and ozone, *Atmos. Environ.*, 101, 294-302, 2015.
- Wexler, A. S., and Clegg, S. L.: Atmospheric aerosol models for systems including the ions H⁺, NH₄⁺, Na⁺, SO₄²⁻, NO₃⁻, Cl⁻, Br⁻, and H₂O, *J. Geophys. Res. -Atmos.*, 107, ACH 14-11-ACH 14-14, 10.1029/2001JD000451, 2002.

15



List of Figures

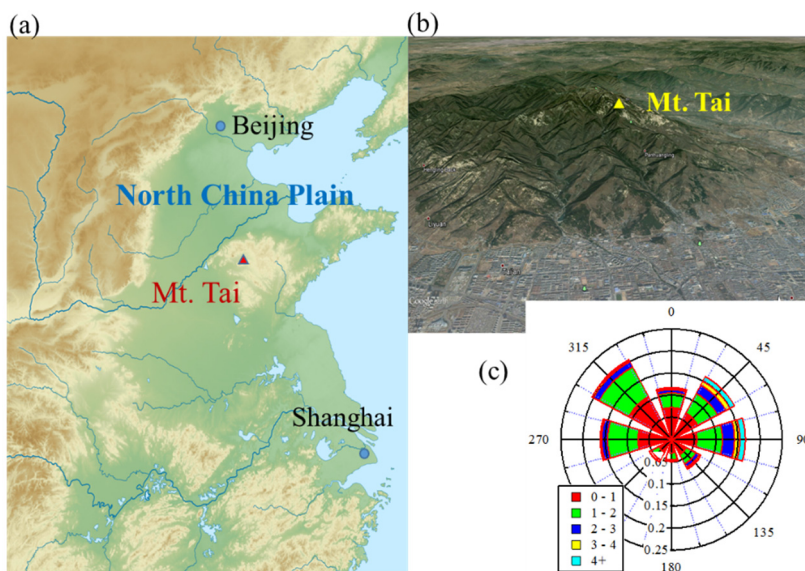
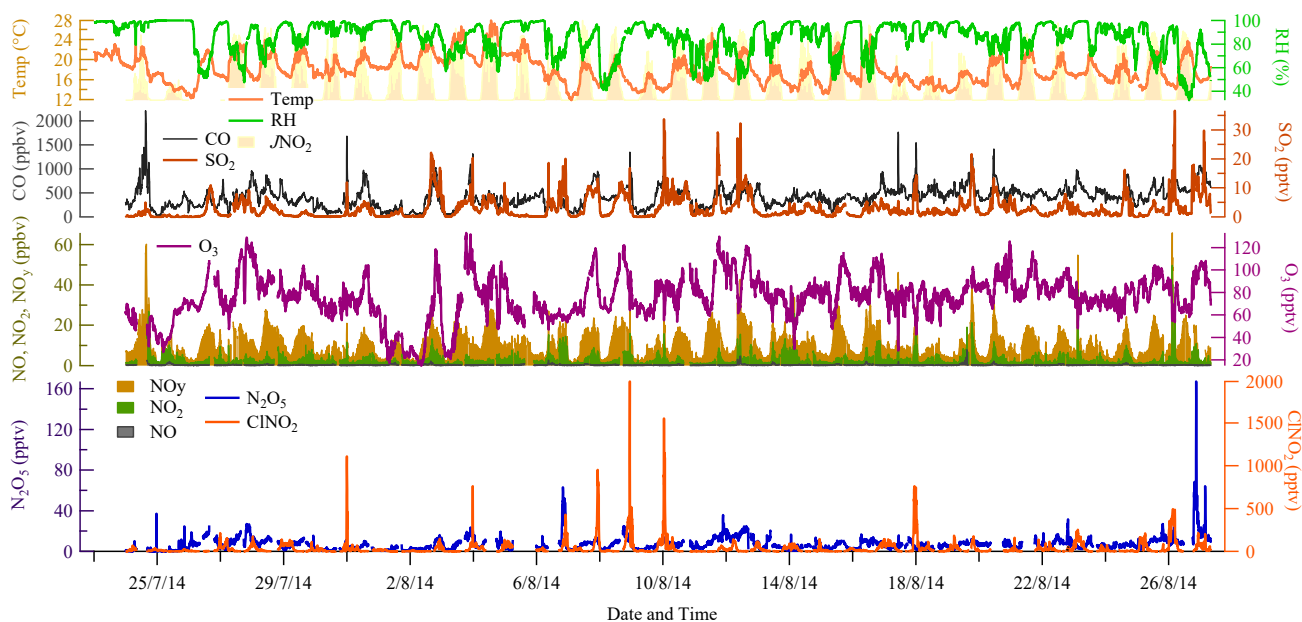
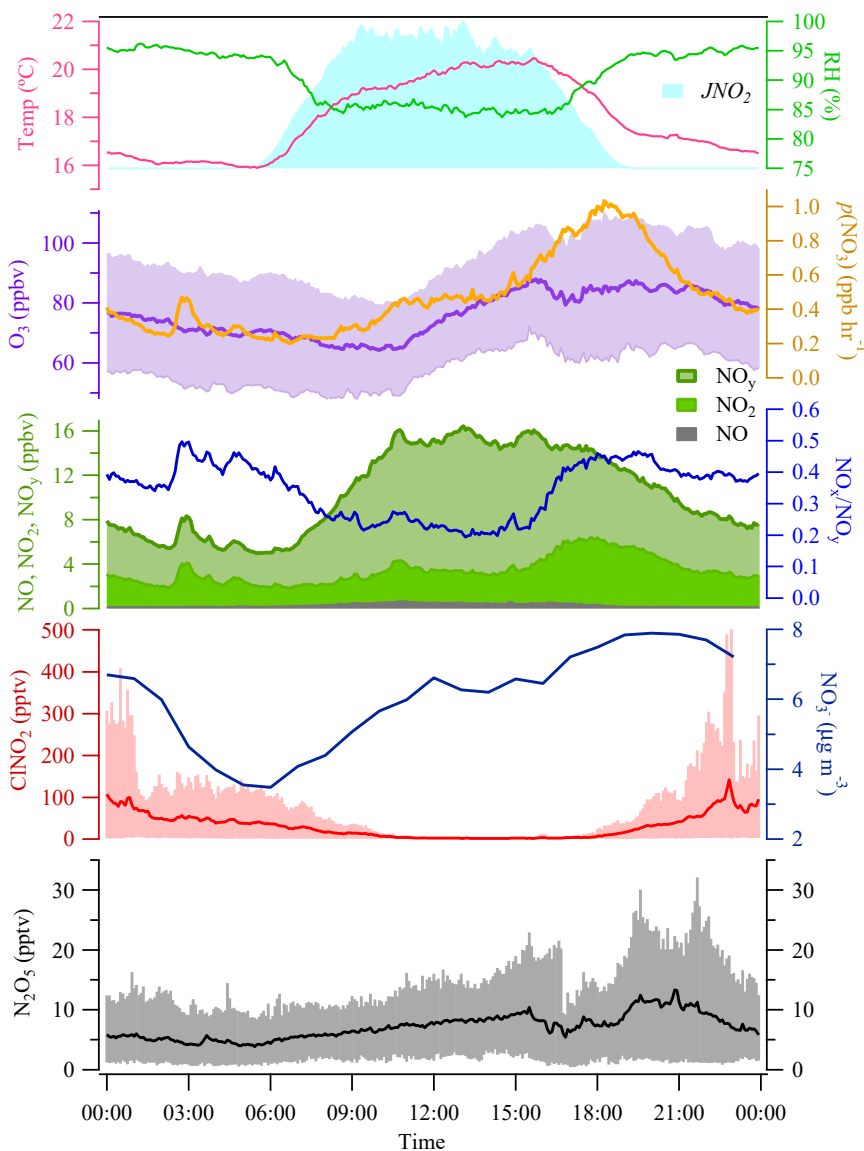


Figure 1: Map of northern China showing the location of the mountaintop measurement site (Mt. Tai) in the North China Plain, and expanded topographic view of Mt. Tai and surrounding areas. The inset shows a wind rose for the study period of summer 2014.



5

Figure 2: Time series (1-min time resolution) for N₂O₅, ClNO₂, related trace gases, and meteorological data measured at Mt. Tai from July 24 to August 27, 2014.



5 **Figure 3: Diurnal variations of N_2O_5 , $ClNO_2$, NO_x , NO_y , O_3 , particulate nitrate, nitrate radical production rate $p(NO_3)$ and meteorological parameters during the study period at Mt. Tai. Shaded area in O_3 shows 2σ variation, and vertical bars in N_2O_5 and $ClNO_2$ represent 10-90th percentile ranges.**

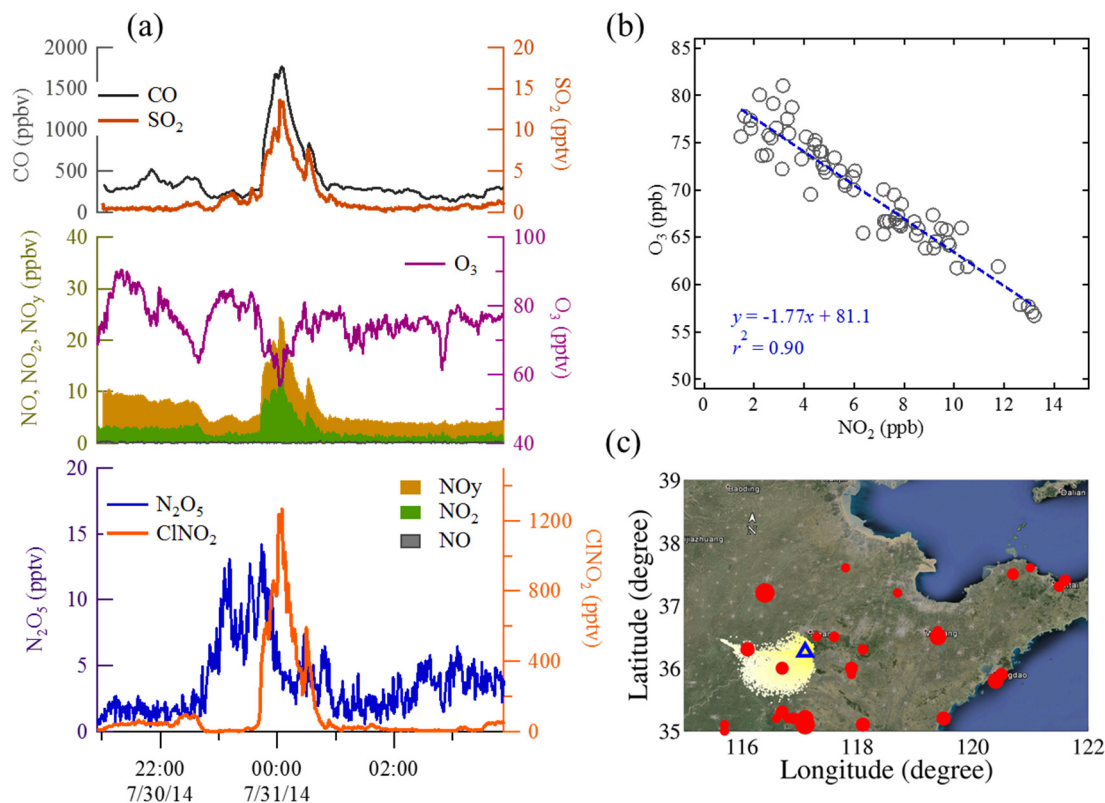


Figure 4: (a) Time series for ClONO₂, N₂O₅, and related trace gases observed within the high-ClONO₂ power plant plume during the night of July 30-31, 2014. (b) Plot of O₃ versus NO₂ concentrations for the power plant plume; plume age was determined from the plot using Eq. (2). (c) 12-h HYSPLIT backward particle dispersion image depicting air masses arriving at the measurement site at the time of the plume, and dots indicating the location of major coal-fired power plants in the region, with the size of dots showing their generation capacities.

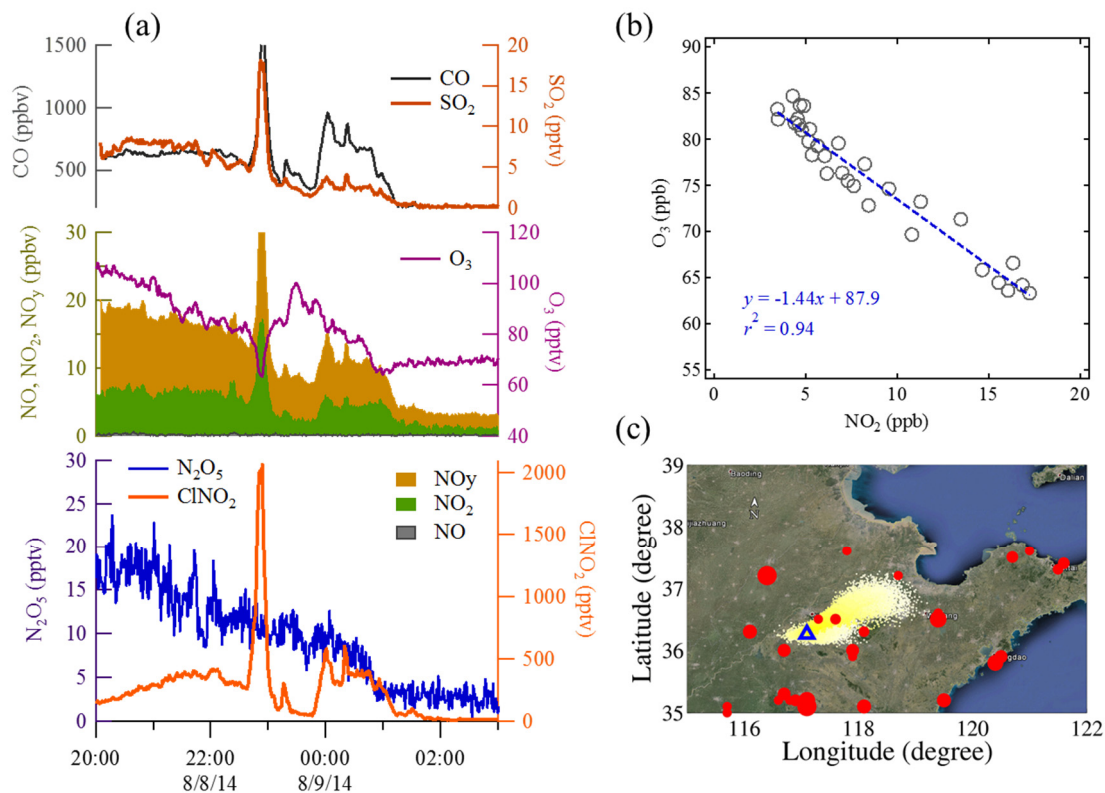


Figure 5: Same as Figure 4 but for a plume observed during the night of August 8-9, 2014.

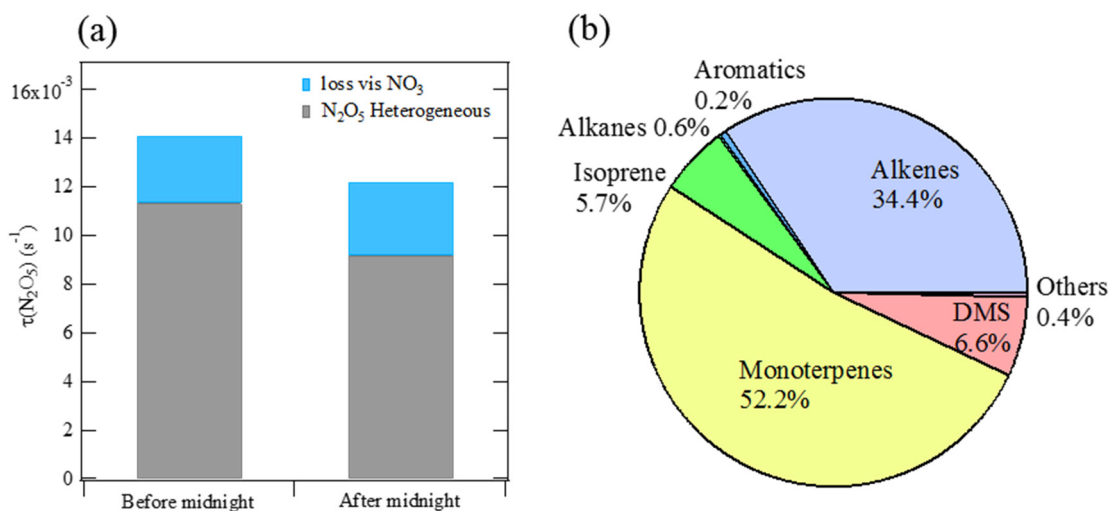


Figure 6: (a) Fractions of N₂O₅ loss rate coefficients through NO₃ loss and the heterogeneous reaction of N₂O₅ before (19:00-24:00) and after midnight (1:00-5:00); (b) pie chart showing the average nighttime contributions of different categories of VOCs to NO₃ reactivity during the study period.

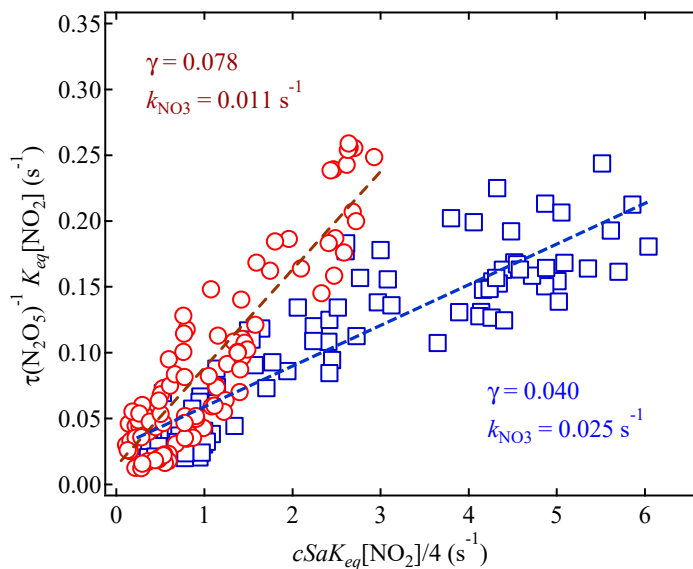


Figure 7: Example fits of inverse N_2O_5 steady-state lifetimes according to Eq. (5) for two cases observed on the nights of August 2 and 21, 2014. The best fit values of γ and k_{NO_3} are shown.

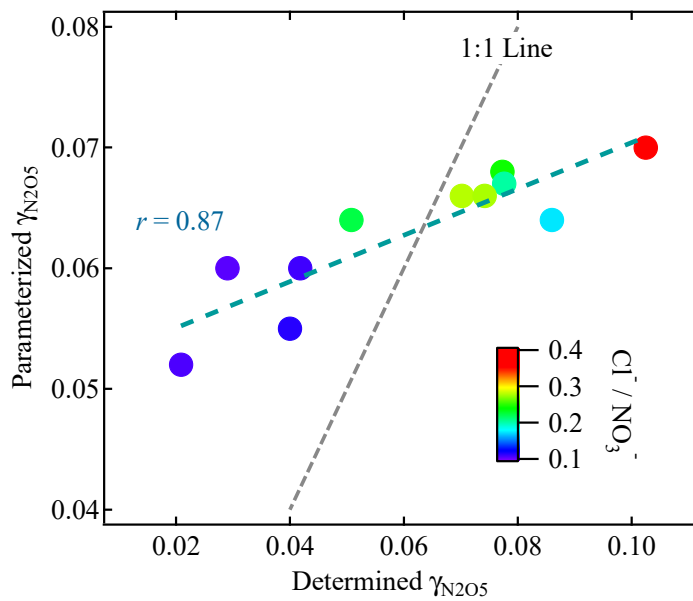


Figure 8: Comparison of field-determined γ with that derived from the parameterization of Bertram and Thornton, (2009). The colors of the markers indicate the corresponding concentrations ratio of particulate chloride to nitrate.

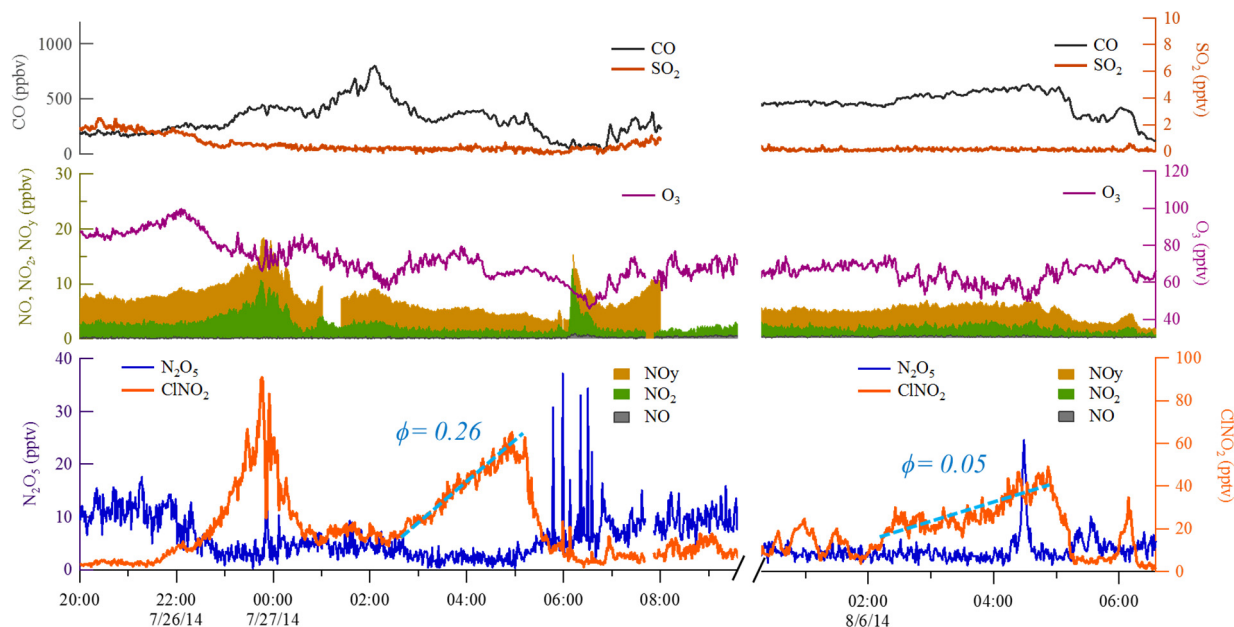


Figure 9: Examples of CINO₂ yields determined for two cases on July 27 and August 6, 2014. The CINO₂ mixing ratios increased steadily, while those of NO_x, O₃, and SO₂ did not change significantly during the studied periods.

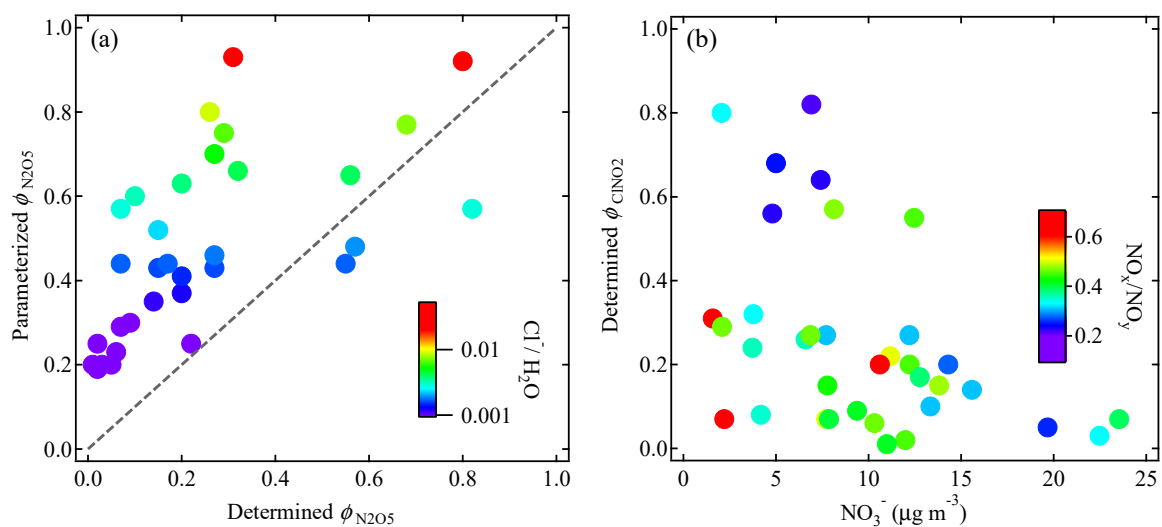


Figure 10: (a) Comparison of field-determined ϕ with that derived from parameterization (Eq. 7), and the colors of the markers represent the corresponding Cl⁻/H₂O ratio; (b) relationship between field-determined ϕ and measure nitrate concentrations in aerosols, and colors of markers represent the corresponding NO_x/NO_y ratio.

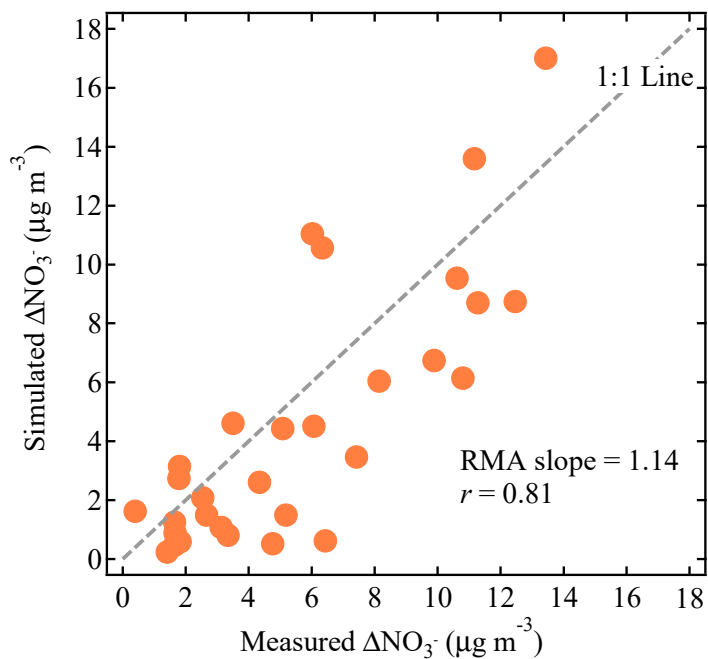
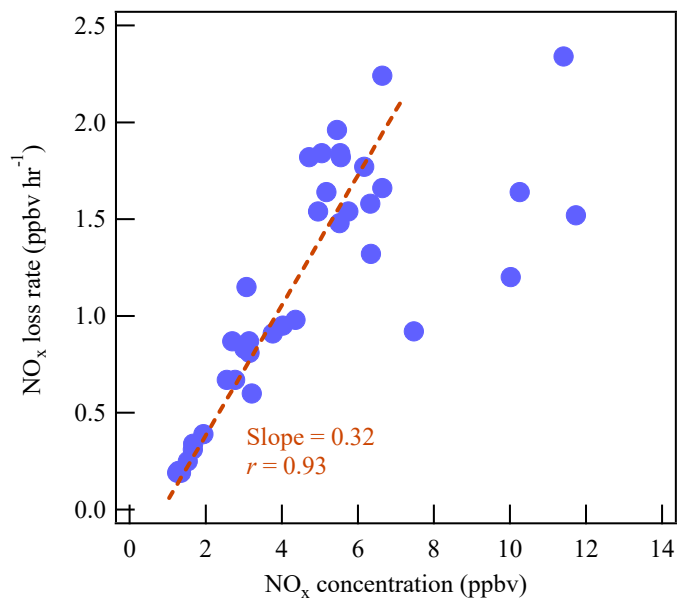


Figure 11: Comparison of predicted nitrate production based on integrating the derived nitrate formation rate with the measured increase in nitrate concentrations (ΔNO_3^-) over the analysis time period.



5 Figure 12: Relationship between determined NO_x loss rate and observed ambient NO_x concentration at the measurement site during the study period.



Table 1: Chemical characteristics of power plant plumes exhibiting high levels of ClNO₂ observed at Mt. Tai during the summer of 2014

| Date | Duration | N ₂ O ₅ (pptv) | | ClNO ₂ (pptv) | | ClNO ₂ /N ₂ O ₅ | O ₃ | NO _x | NO _y | NO _x /NO _y | t _{plume} | φ _{ClNO₂} |
|-----------|-------------|--------------------------------------|---------|--------------------------|---------|--|----------------|-----------------|-----------------|----------------------------------|--------------------|-------------------------------|
| | | Mean | Maximum | Mean | Maximum | | | | | | | |
| 30-31 Jul | 23:40-0:45 | 5.9 | 14.2 | 528 | 1265 | 90 | 70 | 6.5 | 13.2 | 0.49 | 3.2 | 0.57 |
| 3-4 Aug | 23:30-0:00 | 20.1 | 23.8 | 506 | 833 | 25 | 106 | 2.8 | 12.7 | 0.22 | 4.9 | 0.64 |
| 7 Aug | 21:30-23:30 | 10.5 | 14.9 | 606 | 976 | 58 | 91 | 5.8 | 16.3 | 0.36 | 5.5 | 0.35 ^a |
| 8 Aug | 22:00-23:10 | 11.0 | 15.1 | 841 | 2065 | 77 | 76 | 8.5 | 18.8 | 0.45 | 2.1 | 0.90 |
| 8-9 Aug | 23:40-01:15 | 6.8 | 12.6 | 315 | 599 | 46 | 77 | 4.3 | 10.4 | 0.41 | 4.4 | 0.23 |
| 10 Aug | 0:00-2:00 | 10.5 | 15.5 | 692 | 1684 | 66 | 72 | 6.2 | 14.4 | 0.43 | 4.6 | 0.55 |
| 17-18 Aug | 22:00-01:30 | 3.5 | 7.7 | 409 | 802 | 118 | 60 | 9.5 | 17.2 | 0.55 | 4.6 | 0.26 ^a |
| 25-26 Aug | 0:00-5:00 | 12.1 | 40.1 | 301 | 534 | 25 | 74 | 11.8 | 19.1 | 0.62 | 3.0 | 0.20 |

^a For t_{plumes} longer than the nocturnal processing period since sunset, the time since sunset was used in the ClNO₂ yield calculation.

5

Table 2: Statistical summary of determined N₂O₅ uptake coefficients γ, ClNO₂ yields φ, nitrate formation rates and nocturnal NO_x removal rates at Mt. Tai during the study period.

| | γ _{N₂O₅} | k _{NO₃} | φ _{ClNO₂} | NO ₃ ⁻ formation rate (ppt s ⁻¹) | NO ₃ ⁻ formation rate (μg m ⁻³ hr ⁻¹) | NO _x removal rate (ppt s ⁻¹) | NO _x removal rate (ppb hr ⁻¹) |
|--------|---|-----------------------------|-------------------------------|---|---|--|---|
| Mean | 0.061 | 0.015 | 0.27 | 0.29 | 2.2 | 0.31 | 1.12 |
| SD | 0.025 | 0.010 | 0.24 | 0.18 | 1.4 | 0.17 | 0.63 |
| Median | 0.070 | 0.011 | 0.20 | 0.26 | 2.0 | 0.27 | 0.98 |
| Min | 0.021 | 0.003 | 0.02 | 0.02 | 0.2 | 0.05 | 0.19 |
| Max | 0.102 | 0.034 | 0.90 | 0.62 | 4.8 | 0.65 | 2.34 |

10